Transdisciplinary Engineering for Complex Socio-technical Systems
K. Hiekata et al. (Eds.)

doi:10.3233/ATDE190103

Proposal on Miniaturization of Distributed Sensing System Based on Optical Frequency Domain Reflectometry

Victor SHISHKIN[1], Kenji TANAKA and Hideaki MURAYAMA
The University of Tokyo, Japan

Abstract. The main goal of our research is to develop an integrated photonics circuit for sensing system based on Optical Frequency Domain Reflectometry in order to reduce size, weight and cost of current system. In this work we designed, simulated and fabricated Michelson interferometer integrating components such as adiabatic splitter, loop back mirrors, grating couplers and waveguides on total area 150x410 μm of silicon-on-insulator chip. According to simulation results free spectral range of the interferometer is 0.55 nm. Manufacturing variability was taken into account by performing corner analysis.

Keywords. Optical Fiber Sensors, Photonic Integrated Circuits, Structural Health Monitoring, Preventive Maintenance

Introduction

Nowadays some of the most advanced measurement technologies are based on optical fiber sensors. Such sensors are utilizing optical fibers as a sensing element and capable of measuring temperature, strain, vibration, pressure and other physical parameters [1]. Optical fiber sensors have many advantages over conventional electronic sensors. Due to their immunity to electromagnetic interference and fire safety they are widely used in energy and oil & gas industries. Many sensors can be connected in one line of optical fiber and interrogated over distance of tens of kilometers far away from monitoring station. It allows to perform real-time structural health monitoring of large buildings, pipelines, bridges and tunnels [2]. Because of its small size and light weight, they are attractive for application in aerospace. Additional potential for embedding optical fiber sensors into composite materials during fabrication process would also enable the monitoring of composite structures during their whole life cycle.

Optical frequency domain reflectometry (OFDR) is a measurement technique in optical fiber sensing, which enables measurement of strain and temperature distribution along optical fiber with spatial resolution of 1 mm. This unique feature allows to visualize strain fields and temperature gradients, find a shape, bend radius and twists of the fiber. OFDR finds application in carbon fiber structures testing, design and model validation, structural health monitoring and minimally invasive surgical devices. Besides there are many potential applications such as monitoring of temperature distribution in

[1] Corresponding Author, Email: victor@giso.t.u-tokyo.ac.jp.

battery and braking systems of electric vehicles, shape sensing of deployable structures in aerospace, shape and position sensing for feedback system in soft robotics.

However, current OFDR measurement system is too large in size (typically 19-inch-rack mountable), heavy (~10 kg) and fragile, which makes it difficult to install the system on robots, satellites and space rockets, where light weight, small size and robustness are critical requirements. High price of the system doesn't allow it to be used in automobiles and other mass-produced goods.

In order to reduce size and cost of OFDR system we are planning to utilize similar approaches, techniques and manufacturing equipment used in semiconductor industry. Miniaturization and integration of discrete electronic components on a single chip led to increase of mass-production capability, decreased size and cost of electronic devices. Therefore, in the same way we are going to integrate discrete optical components (couplers, mirrors, resonators, etc.) on single silicon-on-insulator chip. On-chip integration of optical systems promises significant cost reduction as well as a variety of new functionalities within compact devices [3, 4], which will greatly expand applicability.

1. Integration of conventional OFDR system

Conventional OFDR system consists of two optical fiber Michelson interferometers (one is for reference and another is for measurement), tunable laser, photodetectors and electronics for signal processing (Figure 1).

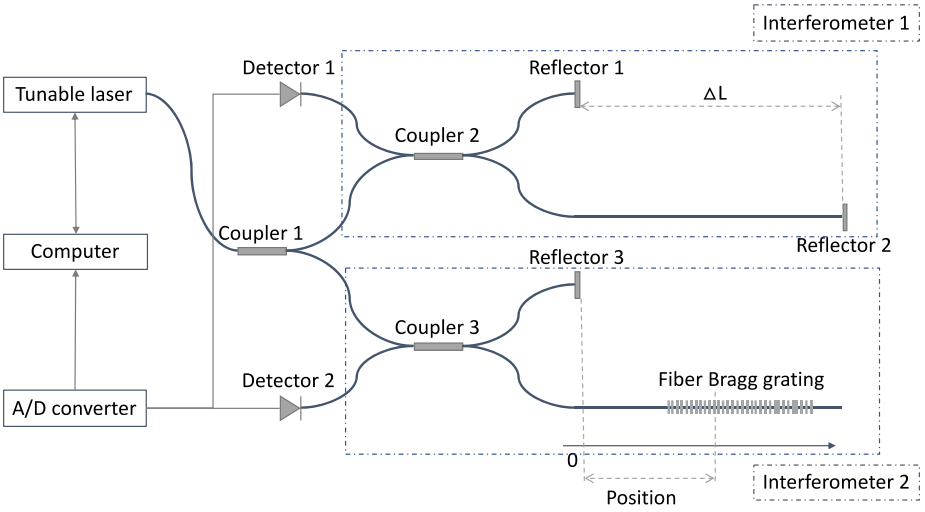

Figure 1. Schematic of OFDR system.

We are starting the integration by replacing optical fiber based interferometers in current system by interferometers implemented on photonic integrated circuits. In further steps we are planning to integrate detection system as well as laser on the same chip with interferometer.

2. Modeling and simulations

2.1. Michelson interferometer theory

Simple model of the Michelson interferometer can be represented as a beam splitter/combiner, two waveguides (with different or equal lengths) and too loopback mirrors. For simplicity we consider lossless waveguides ($\alpha = 0$) and perfect beam splitter/combiner. We will also assume that the waveguides in two arms of the interferometer are identical in terms of the effective index ($\beta_1 = \beta_2$), but have different lengths ($\Delta L = L_2 - L_1$). In case of the ideal beam splitter/combiner (BSC) the electric field intensity of the light wave at the output channels of the BSC should be equal to $I_1 = I_2 = I_i/2$, where I_i is the intensity of the input radiation. It leads to the equation for the electric field $E_1 = E_2 = E_i/\sqrt{2}$. After propagation through the waveguides and reflection from loop back mirrors this fields will accumulate phase shift, which can be represented as:

$$\tilde{E}_1 = E_1 e^{-2i\beta L_1} = \frac{E_i}{\sqrt{2}} e^{-2i\beta L_1}, \quad (1)$$

$$\tilde{E}_2 = E_2 e^{-2i\beta L_2} = \frac{E_i}{\sqrt{2}} e^{-2i\beta L_2}. \quad (2)$$

After passing through BCS again these fields will interfere leading to the output beam intensity:

$$I_0 = \left[\frac{\tilde{E}_1 + \tilde{E}_2}{\sqrt{2}}\right]^2 = \frac{I_i}{4}\left|e^{-2i\beta L_1} + e^{-2i\beta L_2}\right|^2 = \frac{I_i}{2}(1 + \cos(2\beta\Delta L)). \quad (3)$$

Here we take into account that the field at the output of BSC is $E_0 = \frac{E_1 + E_2}{\sqrt{2}}$, where E_1 and E_2 are the electric fields at the input 1 and 2, respectively. Using described above equation we can get the free spectral range (FSR) of the interferometer, which is the spectral spacing between two maxima of the sinusoidal I_0 oscillations (period between two peaks):

$$FSR(\lambda) = \frac{\lambda^2}{2n_g(\lambda)\Delta L} \quad (4)$$

where n_g is the group index of the waveguides.

2.2. Waveguide modeling

Schematic illustration of the waveguide geometry for numerical simulation is shown in Figure 2. Typical strip waveguide made of silicon immersed to the silicon dioxide material is considered. Its height equals 220 nm, while the width is 500 nm. For the numerical simulations Lumerical MODE software was used. Only the first TE-mode of the waveguide is considered.

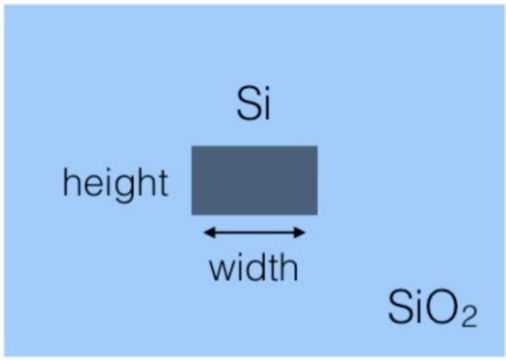

Figure 2. Schematic cross section of the waveguide.

Typical electric field distribution at 1550 nm for the first TE-mode of the waveguide is shown in Figure 3.

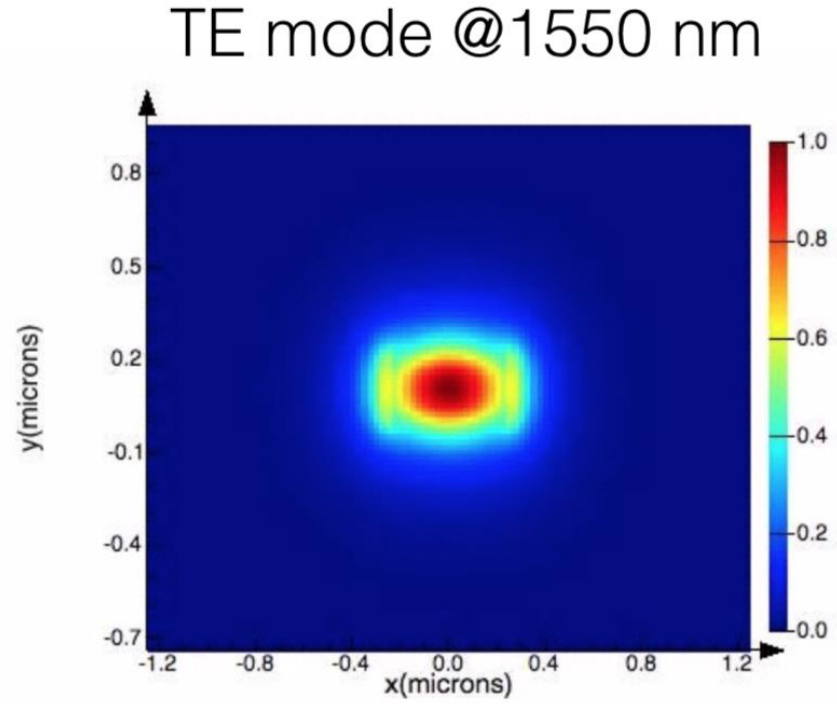

Figure 3. E-field profile in the waveguide (log scale).

Results of the frequency analysis are presented in Figure 4 and 5. These graphs demonstrated results of the numerical simulations for the effective index of the waveguide modes as well as their group index. At the wavelength 1550 nm the effective index equals approximately 2.45 for the TE-mode, the group index equals 4.196.

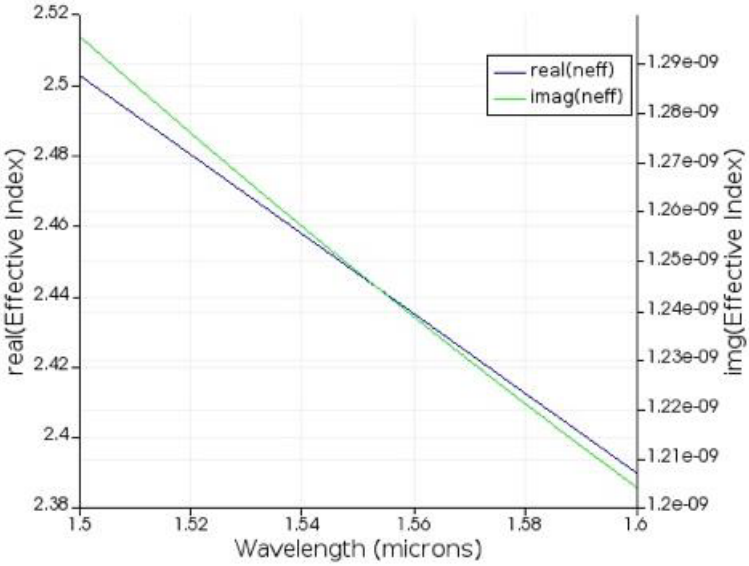

Figure 4. Wavelength dependance of effective index.

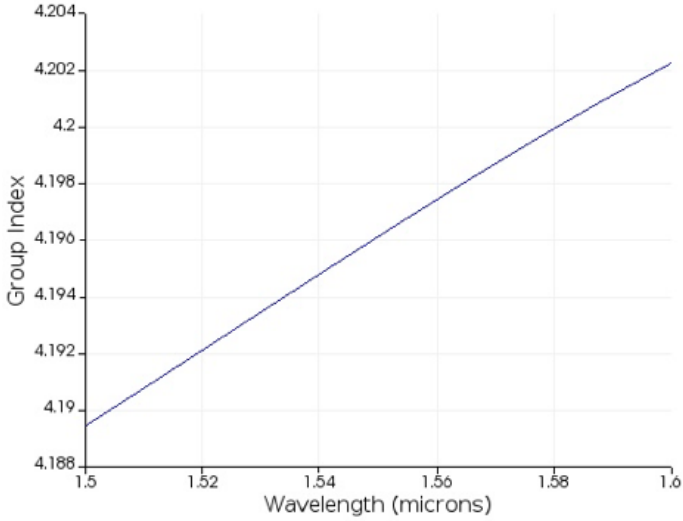

Figure 5. Wavelength dependance of group index.

Applying fitting to the numerical results the compact model of the waveguide can be obtained. The model can be written as Taylor expansion of second order:

$$n_{eff} = 2.446 - 1.129(\lambda - \lambda_0) - 0.042(\lambda - \lambda_0)^2 \qquad (5)$$

for TE-mode of the strip waveguide with width of 500 nm. This analytic expression will serve as a compact model for the circuit simulation.

2.3. Circuit design and simulation

The layout of designed interferometer is presented at Figure 6. The interferometer consists of input and output grating couplers, adiabatic splitter, two strip waveguides with path difference of 600 μm (which makes the interferometer imbalanced) and two loop back mirrors. Total area of the circuit on chip is 150x410 μm.

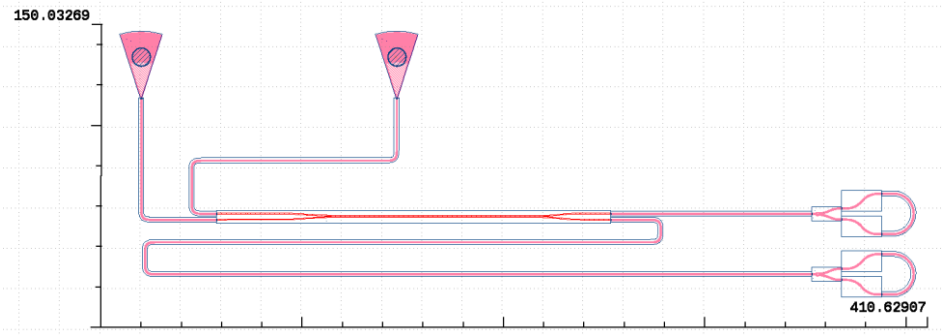

Figure 6. Photonic integrated circuit design of Michelson interferometer.

Numerical simulation for Michelson interferometer is performed using Lumerical INTERCONNECT software. For simulation elements from SiEPIC library [5] are used. Using described in the Michelson interferometer theory section Equation 4 for FSR of the interferometer we can find value of FSR @ 1.55 μm to be 0.48 nm. Numerical result obtained for the case of TE mode is presented in Figure 7. The extracted value of FSR is 0.55 nm, which is in a good accordance with the theoretical predictions achieved above.

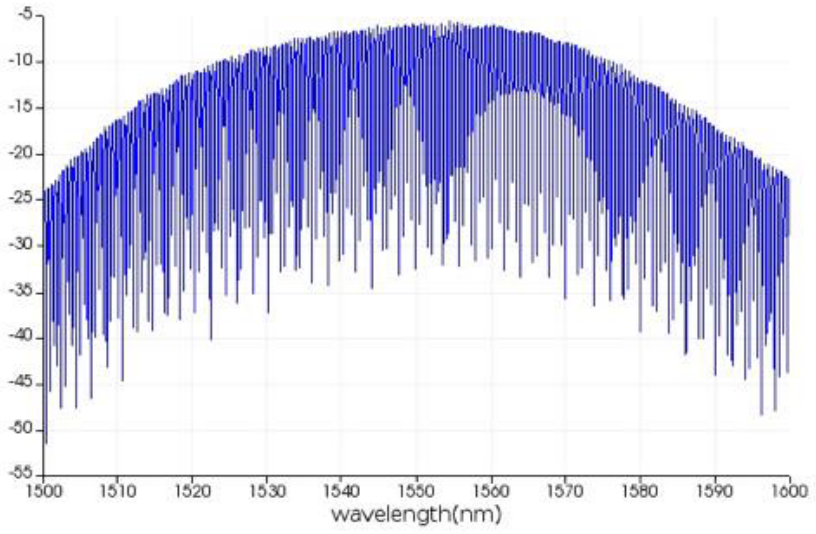

Figure 7. Simulated spectrum of Michelson interferometer on photonic integrated circuit.

3. Fabrication

3.1. Manufacturing variability simulation

In order to take into account manufacturing variability and reduce uncertainty of the circuit performance caused by fabrication process we performed corner analysis, a technique commonly used in semiconductor manufacturing industry. Corner analysis considers typical process variations, such as feature size and threshold voltage variations. These are typically translated into expected device performance (fast or slow transistor). By the analogy with semiconductor manufacturing we will consider possible variations in width and thickness of the waveguide and perform simulations for four extreme cases. Nominal design of the waveguide has dimensions of 500x220 nm. But the wafers we will use are specified 219.2±3.9 nm of silicon layer, so we have to consider waveguide thickness range from 215.3 to 223.1 nm. Waveguide width variation depends on characteristics of resist and electron beam lithography equipment. We will consider a conservative range from 470 to 540 nm. Based on simulation results we calculate group index of the waveguide and expected FSR of the interferometer (Table 1).

Table 1. Corner analysis.

Waveguide width and thickness, nm	Group index	FSR of Michelson interferometer, nm
500x220 (nominal)	4.20	0.48
470x223.1	4.23	0.47
470x215.3	4.24	0.47
540x223.1	4.14	0.49
540x215.3	4.13	0.49

Minimum and maximum group index values are 4.13 (for 540 by 215.3 nm waveguide) and 4.24 (for 470 by 215.3 nm waveguide).

Minimum and maximum values of FSR for Michelson interferometer are 0.47 nm (for 470 by 215.3 nm waveguide) and 0.49 nm (for 540 by 223.1 nm waveguide).

3.2. Fabrication at Takeda super clean room of the University of Tokyo

Michelson interferometer was fabricated on two identical 2x7 mm SOI chips (Figure 8). In fabrication process we used ADVANTEST F7000S-VD02 for electron beam lithography, ULVAC CE-300I for etching, ULVAC SIH-450 for sputtering and DFL7340 for dicing.

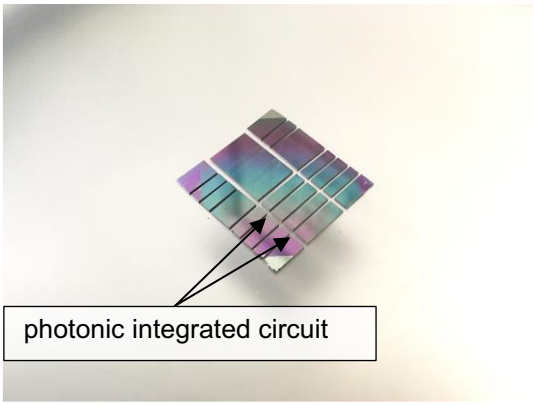

Figure 8. SOI chips with photonic integrated circuit of Michelson interferometer.

4. Conclusions

An integrated Michelson interferometer on photonic integrated circuit is proposed to be used in current sensing system based on Optical Frequency Domain Reflectometry. A prototype of proposed interferometer was designed, simulated and fabricated. Numerical results of simulation for the TE mode of the waveguide as well as results for interferometer are demonstrated. Obtained numerical results will be further compared with results of the experimental characterization.

Acknowledgement

We would like to thank Assoc. Professor Yoshio Mita, Dr. Akio Higo, Dr. Eric Lebrasseur and Mr. Makoto Fujiwara for their support in fabrication of the chip.

References

[1] R. Kashyap, *Fiber Bragg Gratings*, Academic Press, New York, 1999.
[2] B. Glisic and D. Inaudi, *Fibre Optic Methods for Structural Health Monitoring*, John Wiley & Sons, Chichester, (2007).
[3] L. Chrostowski and M.Hochberg, Silicon Photonics Design, Cambridge University Press, Cambridge, 2015.
[4] G.T. Reed and A.P. Knights, *Silicon Photonics An Introduction*, John Wiley & Sons, Hoboken, 2004.
[5] https://github.com/lukasc-ubc/SiEPIC_EBeam_PDK/tree/master/Lumerical_EBeam_CML.